SEMINAR PROCEEDINGS

Edited by E.M. Kiley and V.V. Yakovlev

Seminar web site: **http://www.wpi.edu/+CIMS/IMMG/Seminars/**

A Thermoelastic Model for Microwave Ablation of Concrete

B. Lepers, A. Melcher, G. Link, S. Soldatov, and J. Jelonnek

Institute for Pulsed Power and Microwave and Microwave Technology
Karlsruhe Institute of Technology, Karlsruhe, Germany

The use of high power microwave energy for ablation of contaminated concrete is a promising technique to speed up the dismantling of nuclear power plants. A coupled simulation using Comsol finite element software is performed by solving the electromagnetic wave equation at 2.45 GHz for a standard waveguide and a concrete block. The temperature field is obtained with the heat equation and the microwave power dissipation as a source term. The displacements and stress fields are obtained by solving a thermoelastic model.

Keywords: microwave heating, thermoelasticity, concrete

Introduction

In the near future, Germany will have to dismantle nuclear power plants, and a large amount of contaminated concrete material will have to be removed. High power microwave heating could be used to remove contaminated layers faster than could be done using conventional methods. High power density leads to the development of thermal stress and pore pressure from water vaporization, and eventually results in crack formation and explosive spalling [1, 2]. Analytical estimation of the power density required to achieve a target temperature in 10 and 30 s is given. A coupled thermoelastic model of microwave heating of concrete with constant parameters is presented.

Concrete explosive spalling is due to high thermal stress and possibly pore pressure (up to 4 MPa) [3] from water vaporization. It occurs usually between $150\,^{\circ}\mathrm{C}$ to $300\,^{\circ}\mathrm{C}$ with rapid heating. High temperature gradients inside the concrete material between the heated zone and the colder surrounding concrete are caused by the low thermal conductivity of concrete and a Gaussian power distribution profile type. The power density required to achieve such temperatures inside the concrete material can be estimated from energy conservation. In our experiment the input power is in the range from 5 to 10 kW and the explosive spalling typically occurs after 10 to 30 s. The power densities necessary to elevate the temperature to 150 to $300\ ^{\circ}\mathrm{C}$ for different heating times are shown by the red and green curves in Figure 1.

We make use of the following relation:

$$q \;=\; \frac{\rho C_p \Delta T}{\Delta t}, \tag{1}$$

with density $\rho = 2400\ \frac{\mathrm{kg}}{\mathrm{m}^3}$ and specific heat $C_p = 800\ \frac{\mathrm{J}}{\mathrm{kgK}}$ of concrete. From this power density level ($q_{10s} = 53\ \frac{\mathrm{MW}}{\mathrm{m}^3}$, *i.e.*, a target temperature of $300\ ^{\circ}\mathrm{C}$ in 10 s) and the microwave dissipation losses $P_{\mathrm{em}} = \omega\epsilon_0\epsilon'' E^2_{\mathrm{rms}}$, the electric field can be calculated for dry and wet concrete $\epsilon'' = \{0.1, 0.2, 0.5, 1\}$ at the working frequency $f = 2.45$ GHz:

Table 1: **Power Density Required to Achieve Temperature T $= \{150, 210, 300\}$ °C in 10 and 30 s.**

Power density $[MW/m^3]$	150 °C	210 °C	300 °C
q_{10s}	25	36	53
q_{30s}	8	12	18

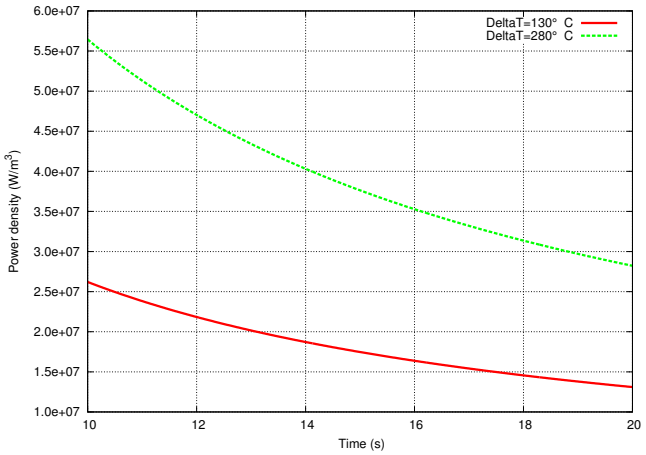

Figure 1: Power density required to elevate the temperature of the concrete from 20 °C to $\{150, 300\}$ °C as a function of time duration.

$$
\begin{aligned}
E_{\text{rms}}^2 &\geq \frac{P_{\text{em}}}{2\pi f \epsilon_0 \epsilon''} \\
E_{\text{rms}} &\geq \sqrt{\frac{53 \times 10^6}{2\pi f \epsilon_0 \{0.1, 0.2, 0.5, 1\}}} \\
&\geq \{63, 44, 28, 20\} \, \frac{\text{kV}}{\text{m}}.
\end{aligned} \tag{2}
$$

From equation 2, wet concrete with a loss factor 10 times higher than dry concrete requires a power density three times less than dry concrete to achieve the same target temperature (the latent heat of water vaporization is not included in the calculation of the temperature).

Material Properties

The main parameter to characterize the propagation of electromagnetic waves and power loss inside a lossy medium is the complex permittivity as shown by the wave equation 3 below. The dielectric permittivity of two different types of concrete was measured at 1.5 GHz, Depending on the water content, the real part of the relative permittivity was in the range $\{5..8\}$[4]. In an other study at 1 GHz, the result was $\epsilon_r{}' = \{4.5..8\}$ and $\epsilon_r{}'' = \{0.1..1.8\}$ for dry and wet concrete [5].

By use of the cavity perturbation method, the dielectric permittivity and loss tangent of few concrete samples were measured at constant frequency $f = 2.45$ GHz as a function of the temperature. The permittivity of the concrete varies by 15 to 20 % in the temperature range 100 to 600 °C once all the water is evaporated as shown in Figure 2. For our simulation, we consider the case of intermediate dry-wet concrete and choose $\epsilon_r = 6 - 0.5j$.

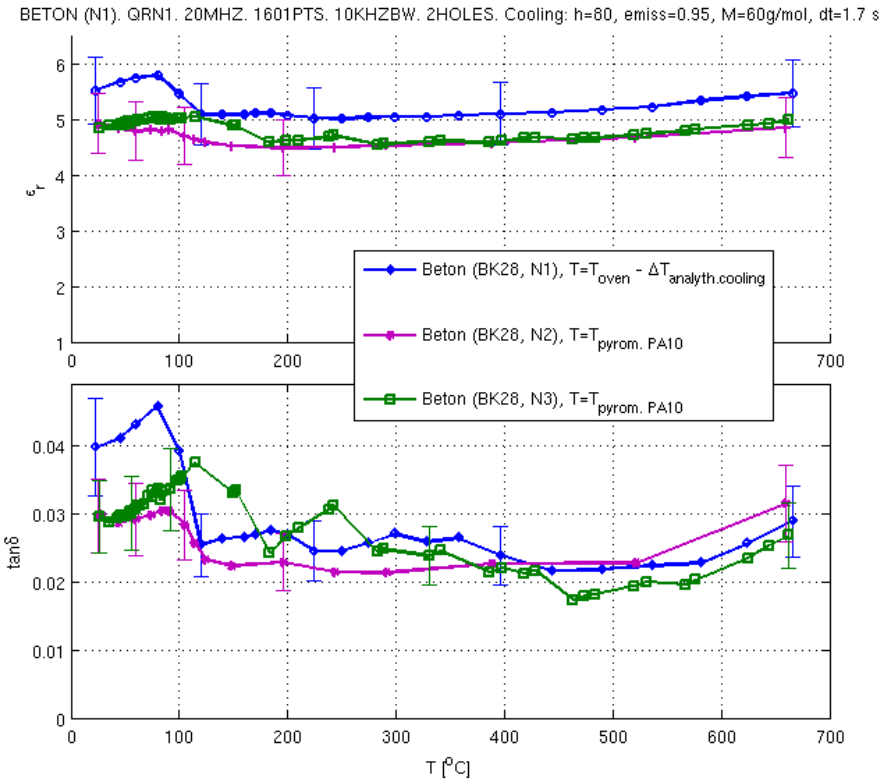

Figure 2: Measured dielectric permittivity and loss tangent of concrete samples at $2.45\,GHz$ as a function of temperature with the cavity perturbation method.

The temperature field can be calculated by solving the transient heat conduction equation. The density $\rho = 2400\ \mathrm{kg/m^3}$, specific heat $c_p = 800\ \mathrm{J/(kg.K)}$ and thermal conductivity $k = 1.7\ \mathrm{W/(m.K)}$ are assumed to be constant; this assumption become less valid when the water content increases.

For small deformations, the concrete material follows an elastic behaviour. Three parameters used in the thermoelastic model define the relationship between the stress $\boldsymbol{\sigma}$ and strain $\boldsymbol{\epsilon}$. The Young's modulus E is a measure of the stiffness of the material, and the Poisson ratio ν is the ratio between transverse and axial strain. The effect of temperature is taken into account with the linear thermal dilatation coefficient α when the solid is subjected to an increase of temperature ΔT. For the simulation, $E = 48\ \mathrm{GPa}$, $\nu = 0.12$ and $\alpha = 10^{-5}\ 1/\mathrm{K}$ are used.

Electromagnetic Model

The antenna is based on a standard WR340 rectangular waveguide. An air gap of $10\ \mathrm{mm}$ is introduced to avoid heat transfer by conduction from the concrete surface to the antenna. The geometry is shown in Figure 3. Due to the vertical plane of symmetry for the electric field, only half of the real geometry is modelled.

The wave equation in free space is obtained from Maxwell's equations:

$$\begin{aligned} \nabla^2\mathbf{E} + \gamma^2\mathbf{E} &= 0 \\ \gamma^2 &= \omega^2\mu\epsilon_0\epsilon_r, \end{aligned} \tag{3}$$

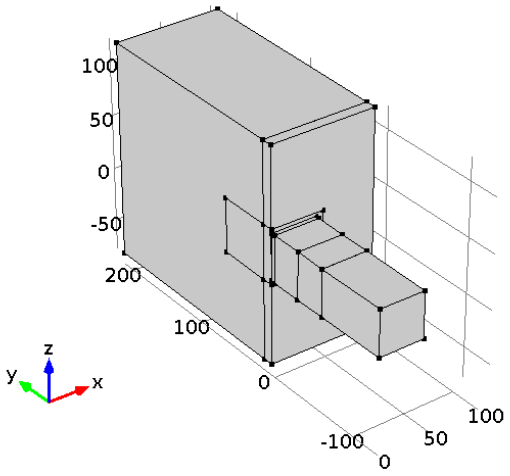

Figure 3: Geometry of the waveguide antenna, air gap and concrete block. The box inside the concrete block is located in front the aperture of the antenna and is a cube of 5 cm length.

where γ is the propagation constant. With the assumption of a homogenous and isotropic medium, we also have $\mathbf{D} = \epsilon\mathbf{E}$, and expressing the wave equation in the frequency domain, the permittivity is a complex number. For our case, all the losses are include in the imaginary part ($\epsilon^{''}$) of the permittivity $\epsilon_r = \epsilon^{'} - j\epsilon^{''}$

The boundary condition on the symmetry plane (the yz-plane in Figure 3) is: $\mathbf{n} \times \mathbf{H} = \mathbf{0}$. At the symmetry plane, only perpendicular magnetic field components exist and in plane electric field components. The wave guide wall is assumed to be a perfect electric conductor, *i.e.*, $\mathbf{n} \times \mathbf{E} = \mathbf{0}$. On the surface of the concrete block, open radiating boundary conditions are applied. With the use of the symmetry boundary condition, only half of the geometry is modelled.

From symmetry, the electric field is a half sinusoid, and is applied on the half port. At 2.45 GHz in our standard WR340 waveguide, only the TE_{10} mode propagates:

$$E_z = \cos\left(\frac{\pi x}{a}\right) \tag{4}$$
$$\beta = \frac{2\pi}{c_0}\sqrt{f^2 - \frac{c_0^2}{4a^2}}$$
$$P_{\text{in}} = \frac{10}{2} = 5 \text{ kW},$$

with c_0 the speed of light, $a = 86.36$ mm the width of the standard WR-340 wave guide, β and P_{in} the propagating constant and the average input power respectively.

The applicator consists of a rectangular wave guide WR-340 with an air gap of 10 mm between the aperture and the concrete surface. At 2.45 GHz the return loss is about -12.7 dB as shown in Figure 4.

Thermal Model

The thermal model solves the heat equation, which is obtained using energy conservation and the Fourier law of conduction as a constitutive relation between heat flux and thermal gradient.

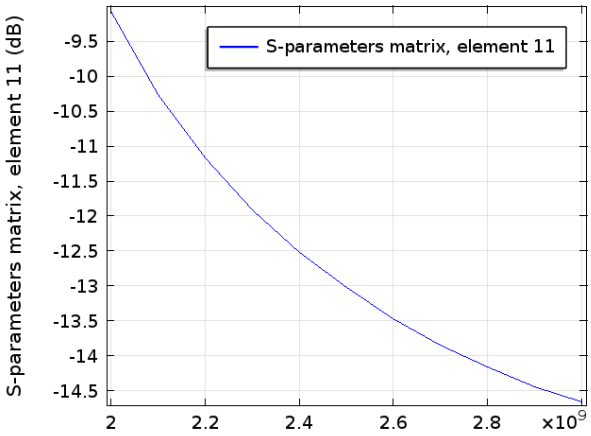

Figure 4: $|S_{11}|_{\text{dB}}$ vs. frequency, air gap 10 mm, $\epsilon_r = 6 - 0.5j$

$$\mathbf{q}(\mathbf{x}, t) = -k\nabla T(\mathbf{x}, t) \tag{5}$$

This law states that for heat propagation inside a solid, the heat flux q is proportional to the thermal gradient. The constant k is the thermal conductivity of the material.

$$\rho c_p \frac{\partial T(\mathbf{x}, t)}{\partial t} = \nabla \cdot (k\nabla T(\mathbf{x}, t)) + q_{em}(\mathbf{x}, t) \tag{6}$$

The temperature field is obtained by solving the heat equation (6). ρ, c_p and k are respectively the density, specific heat and thermal conductivity of the material. q_{em} is the source term, representing power dissipated in microwave heating.

Heating of the concrete block typically occurs during about 10 to 30 s, or until explosive spalling occurs. With this heating time period and low thermal conductivity of the concrete, the temperature inside the concrete is not affected by natural convective cooling by the surrounding air. The adiabatic boundary condition is applied on the surface of the concrete block and on the symmetry plane:

$$\mathbf{n} \cdot \nabla T = 0 \tag{7}$$

Mechanical model

$$\rho\ddot{\mathbf{u}}(\mathbf{x}, t) - \nabla\mathbf{P}(\mathbf{x}, t) - \kappa(\mathbf{x}, t) = 0 \tag{8}$$

The mechanical model is based on force equilibrium (or Newton's law extended to solids) where ρ is the density of the solid, $\mathbf{u}$ is the displacement vector, and $\mathbf{P} \simeq \sigma$ is the material stress tensor for small deformation. $\boldsymbol{\kappa}$ represents the external volume forces such as gravity or magnetic forces. In our case, gravity is negligibly small in comparison to internal thermal stress. In addition, the inertial term $\rho\ddot{\mathbf{u}}$ was neglected, as it is very small in comparison to the thermal stress because the duration of the "heat pulse" (for microwave heating, about 10 s) is much larger than the characteristic time of propagation of stress waves inside the solid (speed of sound in the material over a characteristic length of the

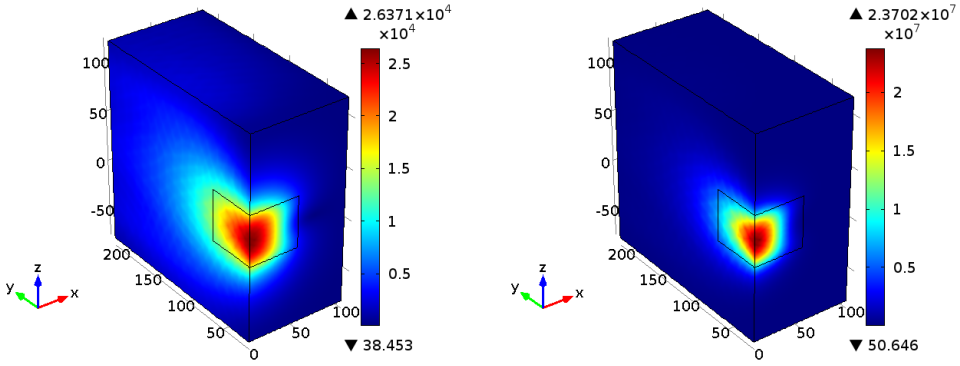

(a) $|\mathbf{E}|$. (b) Q_{h}.

Figure 5: Maximum electric field $|\mathbf{E}|$ and power density Q_{in} in concrete block sample, with $P_{\mathrm{in}} = 10$ kW, $\epsilon = 6 - 0.5j$.

solid). Equation (8) without the inertial term is also called the quasi-static approximation equilibrium of solid.

The constitutive law used to model the concrete material behaviour is a linear elastic model or generalised three-dimensional Hooke's law. This behaviour is realistic in the elastic regime of the material. Three parameters are used to defined the relationship between the strain: $\boldsymbol{\epsilon}$ and $\boldsymbol{\sigma}$ in the case of thermal dilatation, with temperature difference ΔT.

$$\boldsymbol{\sigma} = \frac{E}{1+\nu}\boldsymbol{\epsilon} + \frac{E\nu}{(1+\nu)(1-2\nu)}\,\mathrm{tr}(\boldsymbol{\epsilon})\mathbf{I} - \alpha\frac{E}{1-2\nu}\Delta T\mathbf{I} \tag{9}$$

On all faces of the cube and the symmetry plane, only tangential displacements are allowed, *i.e.*, $\mathbf{n}\cdot\mathbf{u} = 0$ with $\mathbf{n}$ the vector normal to the corresponding face. The face in front the aperture of the waveguide is not constrained, and displacements are allowed in the all three directions.

Results

The model is solved sequentially, with one step corresponding to each physical phenomenon to be modelled, since the dielectric, thermal, and mechanical properties are constant. The power dissipation is calculated with the electromagnetic model at 2.45 GHz and used as an input for the thermal model. Then, the obtained temperature field is used as an input for the thermoelastic model to calculate the displacements and stress fields. The thermal and mechanical model are solved from 0 to 20 s in time steps of 2 s. The elements used for the mesh were tetragonal, and a minimum of 10 elements per wavelength were used inside the domain.

The maximum electric field and power density are $|\mathbf{E}| = 26\,\frac{\mathrm{kV}}{\mathrm{m}}$ and $Q_{\mathrm{em}} = 23\,\frac{\mathrm{MW}}{\mathrm{m}^3}$ as shown in Figures 5a and 5b respectively. At the location of maximum power, the temperature is 136 °C within 10 s. The power density necessary to achieve 150 °C, calculated in Section 1, is $25\,\frac{\mathrm{MW}}{\mathrm{m}^3}$.

The maximum temperatures are located in the center at the exit of the antenna aperture. $T = \{136, 347\}$, °C at $t = \{10, 30\}$ s as shown in Figures 6a and 6b respectively. The Gaussian distribution pattern of the power density and the low thermal conductivity of concrete explains that the highest thermal gradients are located in a ring as shown in Figure 7.

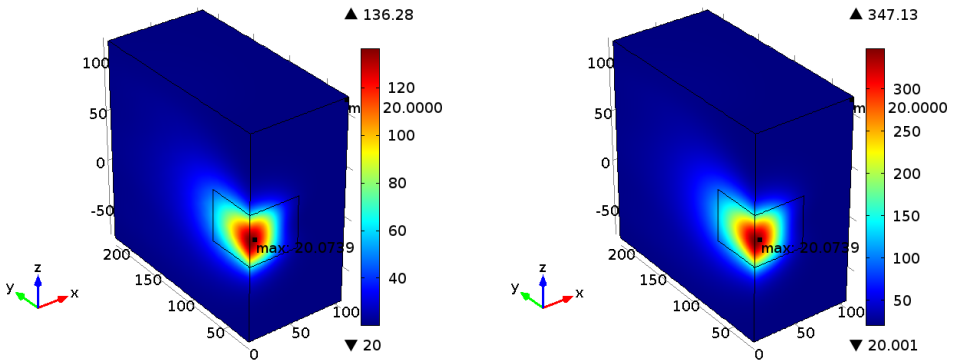

(a) $T(t = 10\text{s})$. (b) $T(t = 30\text{s})$.

Figure 6: Temperature evolution in concrete block sample, with $P_{\text{in}} = 10$ kW, $\epsilon = 6 - 0.5j$.

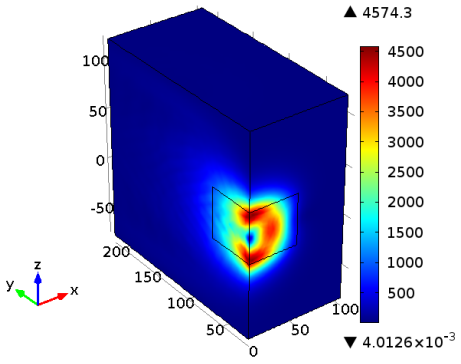

Figure 7: Thermal gradient at $t = 10$ s

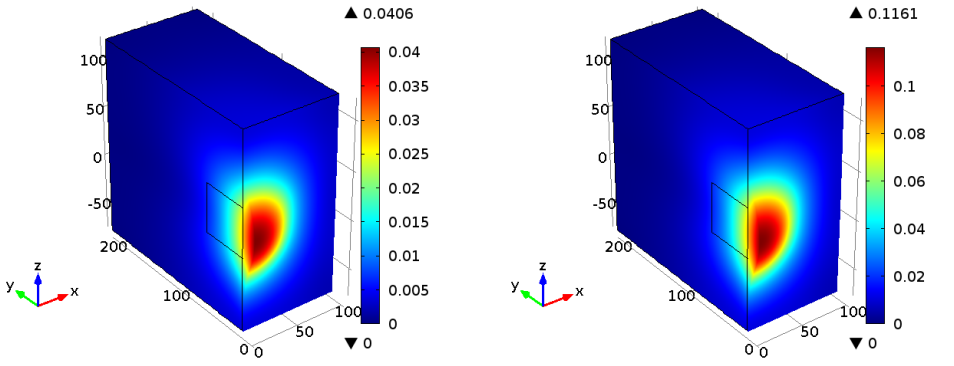

(a) $u(t = 10\text{s})$. (b) $u(t = 30\text{s})$.

Figure 8: Displacement evolution of concrete block sample, $P_{\text{in}} = 10$ kW, $\epsilon = 6 - 0.5j$.

The maximum total displacements are located in the center with $u = \{40, 116\}$ μm at time $t = \{10, 30\}$, s as shown in Figures 8a and 8b.

The maximum von Mises stresses are $\sigma = \{26, 72\}$ MPa at time $t = \{10, 30\}$ s. Figures 9a and 9b show that the stress is maximum along a ring where the highest temperature gradient exists, at the boundary between the heated zone and the colder concrete part. For comparison, the yield strength of

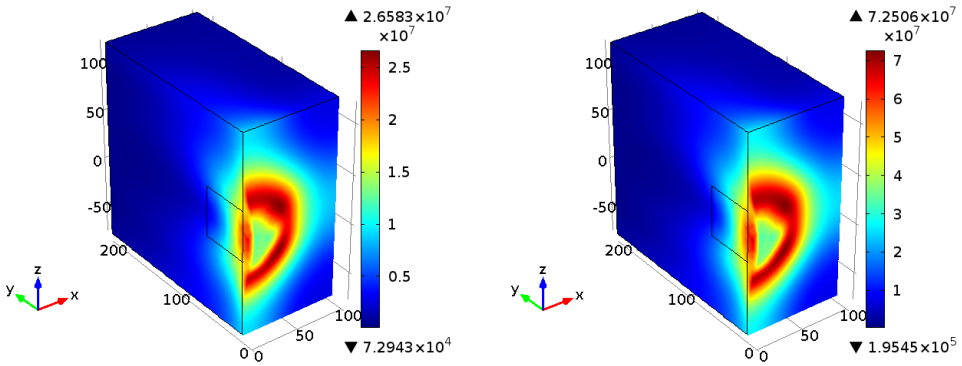

(a) Von Mises ($t = 10$s). (b) Von Mises ($t = 30$s).

Figure 9: Von Mises stress evolution in concrete block sample, $P_{\text{in}} = 10$ kW, $\epsilon = 6 - 0.5j$.

concrete is on the order of 20 MPa depending on the type of concrete.

Conclusion

A COMSOL multiphysics model has been developed that calculates the thermal stress inside a concrete block by running sequentially an electromagnetic, thermal, and mechanical model with constant material properties. The advantage of this model is a minimum number of parameters, a reduced computation time and somewhat realistic results for dry concrete.

For wet concrete in the case of high power microwave heating, its properties are dominated by the water phase change and water movements with vaporization and condensation mechanism [6, 7].

To model the thermal and mechanical behaviour of wet concrete, water transport with phase change should be considered with a porous model, for example. Such models already exist in the literature, with a large number of parameters and increased complexity [1, 2, 8] .

References

[1] D. Gawin, F. Pesavento, and B. Schrefler, "Towards prediction of the thermal spalling risk through a multi-phase porous media model of concrete," *Computer Methods in Applied Mechanics and Engineering*, vol. 195, pp. 5707–5729, October 2006.

[2] B. Schrelfer, G. Khoury, D. Gaswin, and C. Majorana, "Thermo-hydro-mechanical modelling of high performance concrete at high temperature," *Engineering Computations*, vol. 19, no. 0, pp. 786–819, 2002.

[3] A. Akbarnezhad and K. Ong, "Microwave decontamination of concrete," *Magazine of Concrete Research*, vol. 62, pp. 879–885, December 2010.

[4] G. Klysz, J. Balayssac, and X. Ferrieres, "Evaluation of dielectric properties of concrete by a numerical FDTD model of a GPR coupled antenna: Parametric study," *NDTE International*, vol. 41, no. 0, pp. 621–631, 2008.

[5] L. Sandrolini, U. Reggiani, and A. Ogunsola, "Modelling the electrica properties of concrete for shielding effectiveness prediction," *Journal of Physics D: Applied Physics*, vol. 40, no. 0, pp. 5366–5372, 2007.

[6] D. Gawin, F. Pesavento, and B. Schrefler, "What physical phenomena can be neglected when modelling concrete at high temperature? A comparative study, Part 1: Physical phenomena and mathematical model," *International Journal of Solids and Structures*, vol. 48, pp. 1927–1944, 2011.

[7] D. Gawin, F. Pesavento, and B. Schrefler, "What physical phenomena can be neglected when modelling concrete at high temperature? A comparative study, Part 2: Comparison between modes," *International Journal of Solids and Structures*, vol. 48, pp. 1945–1961, 2011.

[8] D. Dincov, K. Parott, and P. K.A., "Heat and mass transfer in two phase porous materials under intensive microwave heating," *Journal of Food Engineering*, vol. 65, no. 0, pp. 403–412, 2004.